high levels of heme *b* and lipid coextracted from the complex. But the heme from HPII passed through the same step and still came out cis. In modified procedures, the first silica column was omitted, and extracts demetalated, esterified by diazomethane, and separated by silica gel HPLC with a total contact time on silica of ca. 12 min. The material from HPII still came out cis, and that from the complex, trans.

Scrutiny of the chromatograms in Figure 1 reveals small components in each extract possibly coincident with the main component of the other. These were always less than 5% of the area of the main component. Recovered amounts were too small to characterize even by visible spectroscopy and their identity remains open. A small amount of chemical isomerization is thus possible, but, under present conditions the main fractions remained distinct.

Present data do not rule out the possibility that the two hemes share a common structure such as an epoxide **6** (Chart I) at some point in their lifetimes. It is not clear why the epoxide would open two ways with such high respective specificity, unless this pertains to an enzyme-catalyzed biosynthetic step or unless the heme pocket environment somehow directs specificity either in situ or during acid acetone extraction. In the absence of direct heme or porphyrin models, there are no precedents for whether the opening would be facile under extraction conditions. Simple alkyl epoxides would not open readily in cold, mildly acidic acetone.

It should be stressed that the absolute configuration at the chiral carbons is still unknown. The isomers refer only to the relative configuration at C12 and C13. Even with gene-amplified proteins, this question is not likely to be answered in the near future.

Experimental Section

Purification of the terminal oxidase from *E. coli* strain MR43L/F152, extraction of the heme, and conversion and isolation of the *trans*-chlorin *d* have been described previously.[2] The source of the HPII catalase was *E. coli* strain UM255. This is a *katE*::*TN10* derivative lacking HPII that has been transformed with *pAMkatE6* which encodes for HPII.[8] The advantage of this system is that more enzyme is produced because the cloned gene is on a high-copy plasmid. The procedure for the isolation of the catalase HPII from bacterial cells has been described.[5] Approximately 200 mg of protein, corresponding to about 2 μmol of heme, formed the starting material for this study. Heme extraction, demetalization, and chlorin purification from the catalase were performed just as for the prosthetic group from the terminal oxidase complex, and in some experiments the manipulations were done in parallel to ensure comparable experimental conditions. In some heme extraction experiments with the catalase, the protein adopted a gellike state unpon exposure to acidic acetone. Unfortunately, this tended to physically entrap heme and lowered the initial yield. In agreement with previous results, HPII was found to contain only a single type of heme group and was free of any detectable heme *b*.[5] In some extraction experiments, the initial low-resolution silica gel column chromatographic separation of the crude extract, which has been previously described,[2] was omitted. This step is not critical for the catalase heme but is quite useful for the heme from the cytochrome complex in order to free it from detergents that stabilize the native enzyme, lipid in the complex, and the endogenous heme *b* prosthetic groups. Chromatographic comparisons on preparations with and without this step indicated that the retention times of either heme were unaffected.

^{1}H NMR spectra were obtained at 500 MHz on a Bruker AM500 spectrometer. Spectral simulations were done with standard Bruker software packages. FT-IR spectra were obtained on dried films of the *cis*-chlorin *d* derived from HPII by using a Bruker IRS88 spectrometer equipped with a microscope accessory. In this mode, the sample was applied as a solution in dichloromethane to a highly polished aluminum mirror and dried, leaving a thin film. The polished surface allows multiple-pass reflection spectroscopy on very small samples. The technique was necessary because of sample limitations in this case. Mass spectra were obtained by using the fast-atom bombardment technique at the Midwest Center of Mass Spectrometry, Department of Chemistry, University of Nebraska-Lincoln.

Acknowledgment. Support of this work was provided in part by Grant GM36264 from the National Institutes of Health (to R.T.). The Midwest Center for Mass Spectrometry is a National Science Foundation Regional Instrumentation Facility supported by Grant CHE-821164. We thank Gayle Newton for culturing some of the cells used in this work.

(8) Mulvey, M. R.; Sorby, P. A.; Triggs-Raine, B. L.; Loewen, P. C. *Gene* **1988**, *73*, 337-345.

Resonance Raman Spectra of Dioxygen Adducts of Cobalt Porphyrin-Imidazole Complexes. Remarkable Spectroscopic Consequences of Hydrogen Bonding of the Coordinated Imidazole and the Lack of an Effect on the Cobalt-Oxygen Linkage

Leonard M. Proniewicz,[1a,b] Alan Bruha,[1b] Kazuo Nakamoto,[1b] Eishin Kyuno,[1c] and James R. Kincaid*,[1b]

Contribution from the Department of Chemistry, Marquette University, Milwaukee, Wisconsin 53233, and Department of Pharmaceutical Science, School of Pharmacy, Hokuriku University, 3, Ho Kanagawa-Machi, Kanazawa 920-11, Japan.
Received March 13, 1989

Abstract: Resonance Raman (RR) spectroscopic studies of O_2 adducts of the imidazole complexes of a highly protected cobalt-porphyrin are reported. Strategic isotopic labeling studies, employing dioxygen isotopomers and selectively deuteriated imidazole analogues, are used to document and interpret the complicated spectral patterns that emerge as a result of complex vibrational coupling of ν(O-O) with internal modes of the trans-coordinated imidazole ligand. In addition, the observed spectral patterns are shown to be dependent upon temperature, imidazole concentration, and the addition of a hydrogen-bond acceptor. These results indicate that hydrogen bonding of the ligated imidazole to other solution components does not lead to differences in the inherent frequency of ν(O-O) but does result in dramatic alterations of the observed spectral patterns as a consequence of differences in vibrational coupling parameters. The implications of these studies for the interpretation of RR spectra of O_2 adducts of cobalt-substituted hemeproteins are discussed.

The essential goal of hemeprotein research remains the elucidation of the structural and electronic factors that control the remarkably varied functional properties of the active-site heme group. The nature and number of axial ligands that the protein

0002-7863/89/1511-7050$01.50/0

presents to the heme group are the major determinants of reactivity. However, even in many cases where histidyl imidazole serves as the axial ligand, wide variation in reactivity is present as a result of subtle differences in disposition of the axial histidylimidazole and/or the presence of nearby residues.

One such secondary control mechanism that has received much attention involves alteration of the properties of the coordinated histidine as a result of hydrogen bonding of the imidazole N–H to other active-site residues or the peptide framework.[2-6] The possible role of such proximal side hydrogen bonding on the stability of O_2 adducts of hemoglobin and myoglobin has been extensively discussed.[5,6] Ideally, direct probes of O_2 structure and bonding may be employed in a comparison of the protein systems with well-designed, carefully controlled model compound studies. While resonance Raman (RR) spectroscopy is a potentially effective probe, application of this technique to the protein systems has led to ambiguous results and conflicting interpretations.

One major obstacle, the inability to observe enhancement of ν(O–O) in the native iron proteins, was overcome by Yu and co-workers, who showed that ν(O–O) is efficiently resonance enhanced in the cobalt-substituted proteins.[7,8] This approach is validated by the fact that these modified proteins retain the gross structural and functional properties of the native systems. Application of this technique to O_2 adducts of cobalt–myoglobin (MbCo) and cobalt–hemoglobin (HbCo) yielded complex vibrational patterns that were originally interpreted in terms of multiple structures and hydrogen bonding of O_2 to the distal histidylimidazole.[7,9]

In a recent paper,[10] we suggested an alternative interpretation of the protein spectra that invoked vibrational coupling of the bound O_2 with internal modes of the proximal (and possibly the distal) histidylimidazole fragment. The plausibility of this interpretation was supported by the results of concurrent and previous[10-13] model compound studies. In that report, we suggested that such vibrational interactions may prove useful as a probe of subtle alterations in structure and bonding at the active site. Herein we report results of studies of O_2 adducts of imidazole-ligated cobalt porphyrins and demonstrate that the formation of hydrogen bonds between the coordinated imidazole and other solution components does not alter the inherent strength of the cobalt–oxygen linkage but does lead to significant changes in the observed vibrational patterns. The similarity of these patterns to those observed for the protein systems[7-10] and the implications for structural interpretations are discussed.

Experimental Section

Compound Preparation. A "jellyfish" porphyrin, 5α,15α-bis[2-(2,2-dimethylpropanamido)phenyl]-10α,20α-(nonanediamidodi-*o*-phenylene)porphyrin, (H_2Azpiv$\alpha\alpha$), was prepared by coupling of 5α,10α,15α,20α-tetrakis(*o*-aminophenyl)porphyrin with nonanedioyl chloride followed by treatment with pivaloyl chloride.[14] H_2Azpiv$\alpha\alpha$-d_8 was prepared by using the same procedure replacing pyrrole and acetic acid by their deuteriated analogues as starting materials. Cobalt complexes of these porphyrins were prepared by reaction of cobaltous chloride with the porphyrin in dry tetrahydrofuran (THF) in the presence of 2,6-lutidine. The complex was purified by chromatography on an alumina column according to procedure of Collman et al.[15]

Imidazole (Im) was purchased from Aldrich Chemical Co. and purified by sublimation prior to deuteriation. 2-Deuterioimidazole (Im-d_1) was synthesized by heating imidazole in deuterium oxide (^2H_2O) at 50 °C overnight. The initial product, 1,2-dideuterioimidazole, was converted to Im-d_1 by rapid exchange of the deuterioimine group (N^2H) for a proton in aqueous solution.[16] 2,4,5-Trideuterioimidazole (Im-d_3) was obtained by heating Im and ^2H_2O in a high-pressure reaction vessel at 250 °C for 72 h[16] followed by ^2H/H exchange of the deuterioimine group in water at room temperature. 4,5-Dideuterioimidazole (Im-d_2) was synthesized from Im-d_3 by heating an aqueous solution of the base at 50 °C for 12 h. ^1H NMR (in C^2HCl_3) was used to confirm deuterium exchange at the desired positions. The deuteriated analogues were found to be >95% deuteriated at the indicated positions with no significant deuteriation at other positions. All bases were sublimed prior to sample preparation for RR measurements.

Tri-*n*-octylphosphine oxide (TNOP) was purchased from Sigma Chemical Co. and used without further purification. Solvents methylene chloride (CH_2Cl_2), its deuteriated analogue ($C^2H_2Cl_2$), and deuteriated chloroform (C^2HCl_3) were purchased from Aldrich Chemical Co. Methylene chloride was purified by refluxing over calcium hydride and then distilled. The $C^2H_2Cl_2$ and C^2HCl_3 were dried with calcium hydride at room temperature.

The gases $^{16}O_2$ (greater than 99%, AmeriGas) and $^{18}O_2$ (~98% ^{18}O, Monsanto Research) were used without purification. Sample of "scrambled" oxygen ($^{16}O_2$:$^{16}O^{18}O$:$^{18}O_2$ = 1:2:1) were prepared by electrical discharge of an equimolar mixture of $^{16}O_2$ and $^{18}O_2$. Ozone produced using this process was decomposed by including activated 4A molecular sieve in the reaction flask. The mixing ratio of oxygen isotopic molecules was determined by Raman spectroscopy.

Spectral Measurements. The RR spectra were recorded on a Spex Model 1403 double monochromator equipped with a Hamamatsu R928 photomultiplier tube and a Spex DM1B computer. Excitation at 406.7 nm was accomplished with a Coherent Model I100-K3 krypton ion laser. Power at the sample was between 5 and 15 mW. A spectral band-pass of 4 cm^{-1} was routinely used.

Spectral measurements were carried out by using the "minibulb" technique.[17] Concentration studies were conducted by transferring precise volumes of a CH_2Cl_2 solution of known concentration of Im to the minibulb. The solvent was vacuum stripped from the partially frozen solution. The cobalt porphyrin was then added, and the sample was prepared following well-documented procedures[10-13] employing $C^2H_2Cl_2$ as the solvent. A CT Model 21 closed-cycle helium refrigerator was used to maintain samples at the desired temperature during measurements. The exact temperature of the sample was calculated from the measured ratio of intensities of Stokes and anti-Stokes Raman bands of the solvent.[18] Accuracy of the frequency readings was ±1 cm^{-1}.

Results and Discussion

As will be made evident in the following discussion, the O_2 adducts of the imidazole complexes of cobalt porphyrins exhibit complicated RR spectral patterns characterized by multiple oxygen-isotope-sensitive features. These are interpreted with the aid of strategic isotopic labeling experiments and well-controlled variation of solution conditions. In addition, we have employed the cobalt complex of a highly protected porphyrin, i.e., 5α,15α,-bis[2-(2,2-dimethylpropanamido)phenyl]-10α,20α-(nonanediamidodi-*o*-phenylene)porphyrin, abbreviated Co$Az_{piv}\alpha\alpha$ (structure 1). The use of this protected porphyrin minimizes association (and vibrational coupling)[11] of the bound dioxygen with excess imidazole in the solution, thereby allowing attention to be focused on interactions with the trans-axial-coordinated imidazole.

Documentation of vibrational interactions of O_2 with this trans-axial ligand is most effectively accomplished with the use

(1) (a) Permanent address: Regional Laboratory of Physicochemical Analyses and Structural Research, Jagiellonian University, Cracow, Poland. (b) Marquette University. (c) Hokuriku University.
(2) O'Brien, P.; Sweigart, D. A. *Inorg. Chem.* **1985**, *24*, 1405.
(3) Quinn, R.; Mercer-Smith, J.; Burstyn, J. N.; Valentine, J. S. *J. Am. Chem. Soc.* **1984**, *106*, 4136.
(4) Hagen, K. I.; Schwab, C. M.; Edwards, J. O.; Jones, J. G.; Lawler, R. G.; Sweigart, D. A. *J. Am. Chem. Soc.* **1988**, *110*, 7024.
(5) Valentine, J. S.; Sheridan, R. P.; Allen, L. C.; Kahn, P. C. *Proc. Natl. Natl. Acad. Sci. U.S.A.* **1979**, *76*, 1009.
(6) Traylor, T. G.; Popovitz-Biro, R. *J. Am. Chem. Soc.* **1988**, *110*, 239.
(7) Tsubaki, M.; Yu, N.-T. *Proc. Natl. Acad. Sci. U.S.A.* **1981**, *78*, 3581.
(8) Yu, N.-T.; Kerr, E. A. In *Biological Applications of Raman Spectroscopy*; Spiro, T. G. Ed.; Wiley-Interscience: New York, 1987; Vol. 3, p 39.
(9) Kitagawa, T.; Ondrias, M. R.; Rousseau, D. L.; Ikeda-Saito, M.; Yonetani, T. *Nature (London)* **1982**, *298*, 869.
(10) Bruha, A.; Kincaid, J. R. *J. Am. Chem. Soc.* **1988**, *110*, 6006.
(11) Bajdor, K.; Kincaid, J. R.; Nakamoto, K. N. *J. Am. Chem. Soc.* **1984**, *106*, 7741.
(12) Kincaid, J. R.; Proniewicz, L. M.; Bajdor, K.; Bruha, A.; Nakamoto, K. *J. Am. Chem. Soc.* **1985**, *107*, 6775.
(13) Proniewicz, L. M.; Nakamoto, K.; Kincaid, J. R. *J. Am. Chem. Soc.* **1988**, *110*, 4541.
(14) Uemori, Y.; Miyakawa, H.; Kyuno, E. *Inorg. Chem.* **1988**, *27*, 377.
(15) Collman, J. P.; Brauman, J. I.; Doxsee, K. M.; Halbert, T. R.; Hayes, S. E.; Suslick, K. S. *J. Am. Chem. Soc.* **1978**, *100*, 2761.
(16) Grimmett, M. R. In *Comprehensive Heterocyclic Chemistry: The Structure, Reaction, Synthesis and Uses of Hetercyclic Compounds*, Potts, K. T., Ed.; Pergammon Press: Oxford, 1984; Vol. 5, p 416.
(17) Nakamoto, K.; Nonaka, Y.; Ishiguro, T.; Urban, M. W.; Suzuki, N.; Kozuka, M.; Nishida, Y.; Kida, S. *J. Am. Chem. Soc.* **1982**, *104*, 3386.
(18) Strommen, D. P.; Nakamoto, K. In *Laboratory Raman Spectroscopy*; Wiley-*Interscience*: New York, 1984; p 53.

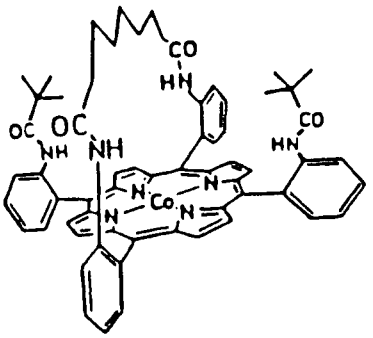

of selectively deuteriated imidazole analogues which alter vibrational coupling interactions while maintaining the chemical integrity of the system. To properly interpret the resulting spectra of the various imidazole isotopomer complexes, it is necessary to document the changes in the imidazole internal modes upon selective deuteriation. Therefore, before proceeding to the discussion of the O_2 adducts, the spectra of the imidazoles are presented and discussed.

A. Raman Spectra of Imidazole and Deuteriated Analogues. The Raman spectra of imidazole and its deuteriated analogues (as solutions in C^2HCl_3) are shown in Figure 1. Only the carbon-deuteriated analogues were used, the N–H proton being retained so as not to introduce any chemical differences. As is evident, all of these analogues exhibit bands between 1050 and 1150 cm^{-1} (i.e., in the ν(O–O) region) and thereby provide opportunities for vibrational coupling of ν(O–O) with internal modes of the base ligands. In the cases of Im (trace A) and Im-d_1 (trace B) a strong polarized band occurs near 1140 cm^{-1}. In trace C it is seen that the strongest feature shifts down to 1118 cm^{-1} for Im-d_2 while a relatively strong doublet is exhibited by Im-d_3 (trace D). In addition to these strong features, the Im and Im-d_1 analogues exhibit weak polarized bands at 1068/1063 cm^{-1} (doublet) and 1088 cm^{-1}, respectively. The 1098-cm^{-1} feature in the spectrum of Im (trace A) is a non-totally symmetric (depolarized) band and is not expected to couple with the polarized ν(O–O). It is especially important to note that in the cases of Im-d_2 (trace C) and Im-d_3 (trace D) there is no evidence for the presence of bands below ~1100 cm^{-1}. Thus, in these cases, there is apparently no opportunity for coupling with $\nu(^{18}O-^{18}O)$, whose natural frequency is expected to occur near 1075 cm^{-1} (vide infra).

This set of spectra confirms the fact that imidazole and its deuteriated analogues exhibit a number of bands in the ν(O–O) region. Furthermore, these data demonstrate that it is possible to alter the vibrational frequencies via selective deuteriation and thereby alter the specific coupling interactions so as to gain insight into the spectroscopic behavior of vibrationally coupled bound dioxygen.

Unfortunately, several factors prevent a straightforward prediction of the possible coupling interactions. First, the spectra shown in Figure 1 are those of noncoordinated imidazoles. In the absence of an effective enhancement mechanism, the natural frequencies of heme-coordinated imidazole are not directly available. It may be expected that the general intensity patterns would persist in the spectra of the coordinated species but that coordination-induced frequency shifts may occur. Indeed, the few reports of Raman spectra of imidazole complexes support this expectation. Thus, Salama and Spiro report that an imidazole mode observed at 1142 cm^{-1} (in acetone) shifts up to 1149 cm^{-1} upon coordination to Co(II).[19] Similarly, Walters and Spiro[20a] as well as Asher and co-workers[20b] report shifts of a free imidazole modes at ~1137 and ~1100 cm^{-1} (H_2O solution) to 1142 and 1109 cm^{-1} upon coordination to $[Fe^{III}(CN)_5]^{2-}$. Comparable shifts of infrared bands in this region have been reported for imidazole complexes of several transition metals.[21] Thus, at least in the case of natural-abundance imidazole, internal modes in this region may be expected to shift up by 5–10 cm^{-1} upon coordination.

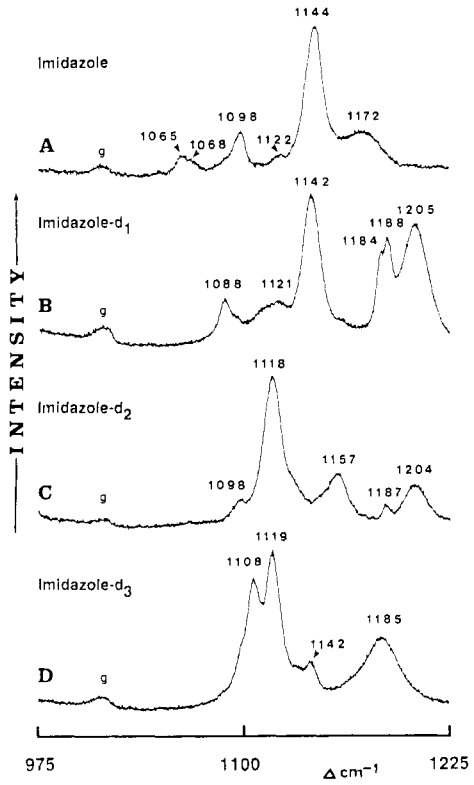

Figure 1. Raman spectra of imidazole and deuteriated analogues. Solutions in C^2HCl_3, ~2–3 M, 514.5-nm excitation, 150 mW at the sample, spinning NMR tube with line focusing (cylindrical lens), room temperature.

In addition to coordination-induced shifts, the internal modes of imidazole may also be sensitive to hydrogen-bond interactions involving the NH, either through self-association[22] or association with other solution components.[22-24] The spectra shown in Figure 1 were obtained at high concentrations of imidazole and represent self-associated species.[22] At concentrations sufficiently low to eliminate self-association, high-quality Raman spectra could not be obtained.

In summary of this section, the Raman spectra of each of the imidazole analogues exhibit one or two strong and several weak bands in the ν(O–O) region that may vibrationally couple with ν(O–O). However, the spectra shown in Figure 1 serve only as an approximate guide for interpretation of the spectra of the O_2 adducts inasmuch as the frequencies of the internal ligand modes may shift upon coordination to the Co(II) porphyrin[19,20] and are also expected to be sensitive to association with excess imidazole in solution[22-24] (vide infra). Nevertheless, as will be shown in the next sections, a knowledge of the approximate frequencies of the internal modes of the various deuteriated imidazoles, taken together with the expectation of coordination- and association-induced shifts derived from previous studies,[19-24] permits a self-consistent analysis of the observed RR spectra of the various O_2 adducts.

B. Resonance Raman Spectra of O_2 Adducts. 1. Vibrational Coupling of ν(O–O) with Internal Modes of Imidazoles. The RR spectra of the O_2 adducts of the imidazole complex of $CoAz_{piv}\alpha\alpha$ are given in Figure 2. The spectrum of the $^{16}O_2$ adduct (trace A) exhibits two lines at 1158 and 1138 cm^{-1}. This spectrum was obtained in $C^2H_2Cl_2$ to eliminate interference by the 1156-cm^{-1}

(19) Salama, S.; Spiro, T. G. *J. Am. Chem. Soc.* **1978**, *100*, 1105.
(20) (a) Walters, M. A.; Spiro, T. G. *Inorg. Chem.* **1982**, *22*, 4014. (b) Jones, C. M.; Johnson, C. R.; Asher, S. A.; Shepherd, R. E. *J. Am. Chem. Soc.* **1988**, *107*, 3772.
(21) Hodgson, J. B.; Percy, G. C.; Thornton, D. A. *J. Mol. Struct.* **1980**, *66*, 81.
(22) Anderson, D. M. W.; Duncan, J. L.; Rossotti, F. J. C. *J. Chem. Soc.* **1961**, 2165.
(23) Perchard, C.; Novak, A. *J. Chem. Phys.* **1968**, *48*, 3079.
(24) Wang, S.-M. J. Lee, L.-Y.; Chen, J.-T. *Spectrochim. Acta* **1979**, *35A*, 765.

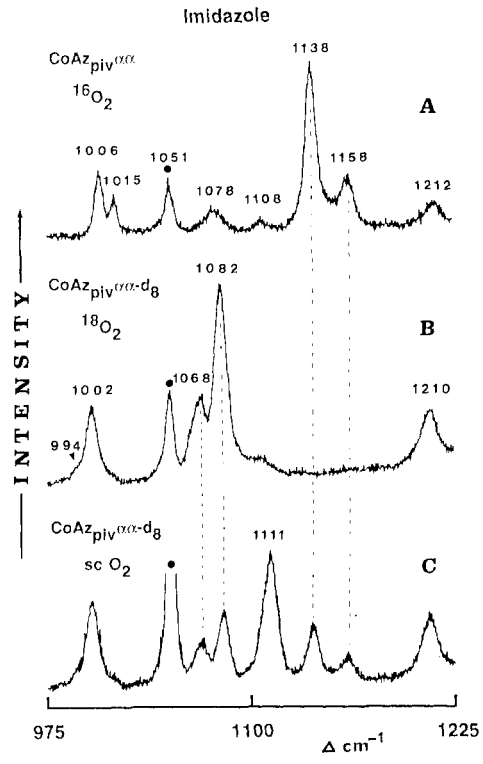

Figure 2. Resonance Raman spectra of O_2 adducts of CoAz$_{piv}^{\alpha\alpha}$ complex with imidazole. Conditions as in text. The 1051-cm^{-1} line (●) is due to $C^2H_2Cl_2$.

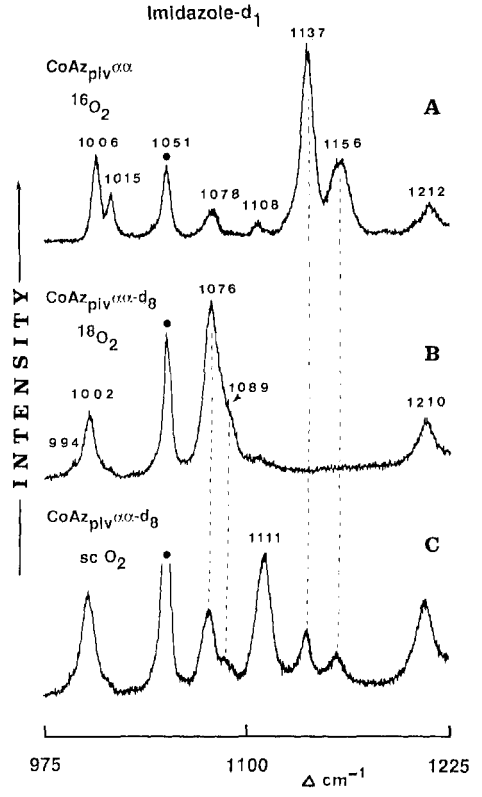

Figure 3. Resonance Raman spectra of O_2 adducts of CoAz$_{piv}^{\alpha\alpha}$ complex with imidazole-d_1. See Figure 2 caption.

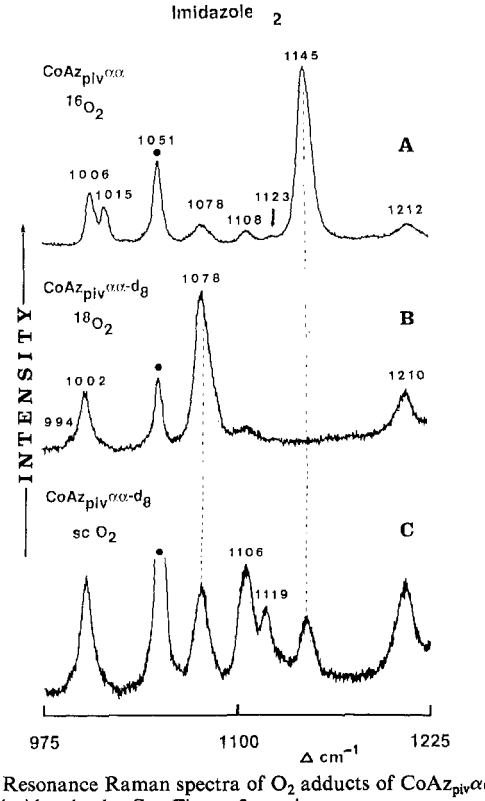

Figure 4. Resonance Raman spectra of O_2 adducts of CoAz$_{piv}^{\alpha\alpha}$ complex with imidazole-d_2. See Figure 2 caption.

(CH_2Cl_2) solvent band. The band at 1051 cm^{-1} is due to $C^2H_2Cl_2$. Porphyrin bands are observed at 1212, 1108, 1078, 1015, and 1006 cm^{-1}. The spectrum of the $^{18}O_2$ adduct is shown in trace B. In this case, the β-pyrrole deuteriated porphyrin is utilized to avoid overlap of the $\nu(^{18}O-^{18}O)$ with the porphyrin mode at 1078 cm^{-1} (see in trace A). The 1078-cm^{-1} mode is extremely sensitive to β-pyrrole deuteriation and shifts out of this region in the case of the pyrrole-deuteriated porphyrin. As can be seen in trace B, two new bands appear at 1068 and 1082 cm^{-1} in the spectrum of the $^{18}O_2$ adduct, the higher frequency component showing the greater intensity. Although the appearance of two bands in the $\nu(^{16}O-^{16}O)$ (trace A) and two bands in the $\nu(^{18}O-^{18}O)$ (trace B) regions may suggest the presence of two structural conformers, the results shown in trace C demonstrate that this cannot be the correct interpretation. In this case (trace C) the solution contains the $^{16}O_2$, $^{18}O_2$, and $^{16}O^{18}O$ adducts. The strong symmetric feature at 1111 cm^{-1} is readily assigned to $\nu(^{16}O-^{18}O)$, i.e., there is no evidence for the presence of a second conformer. Instead, the appearance of multiple bands in the $^{16}O_2$ and $^{18}O_2$ adducts is the result of vibrational coupling of $\nu(^{16}O-^{16}O)$ and $\nu(^{18}O-^{18}O)$ with different internal modes of coordinated imidazole.

The validity of this interpretation is supported by comparison of the corresponding spectra obtained with the deuteriated analogues of imidazole. These spectra are shown in Figures 3–5. In the case of the C_2-deuteriated analogue (Im-d_1, Figure 3), the spectrum of the $^{16}O_2$ adduct (trace A) is seen to be almost identical with that shown for the natural-abundance imidazole complex (Figure 2A). However, the $\nu(^{18}O-^{18}O)$ region (Figure 3B) shows substantial changes compared to Figure 2B, namely, the 1068/1082 cm^{-1} (strong) pair is replaced by bands at 1076 (strong) and (shoulder) 1089 cm^{-1}. The $\nu(^{16}O-^{18}O)$ again appears as an isolated symmetric band at 1111 cm^{-1} (Figure 3C).

A different vibrational pattern is observed for the adducts of complexes bearing axial ligated [4,5-$^2H_2$]imidazole (Im-d_2) and [2,4,5-$^2H_3$]imidazole (Im-d_3) (Figures 4 and 5). The spectra of the $^{16}O_2$ adducts exhibit strong symmetric bands near 1145 cm^{-1} having weak secondary features at lower frequencies (1123 cm^{-1} in Figure 4A; 1115 and 1127 cm^{-1} in Figures 5A; see insert). The $\nu(^{18}O-^{18}O)$ regions in these two cases exhibit strong symmetric bands at 1078 cm^{-1} and no weak secondary features. On the other hand, the $\nu(^{16}O-^{18}O)$ region is remarkably altered for these two cases (Figures 4C and 5C) relative to the spectra shown in Figures 2C and 3C.

It is important to emphasize that chemically innocuous deuteriation has been employed. These analogues have identical chemical reactivity and therefore, *in the absence of vibrational interaction*, are expected to yield identical spectra. The complex

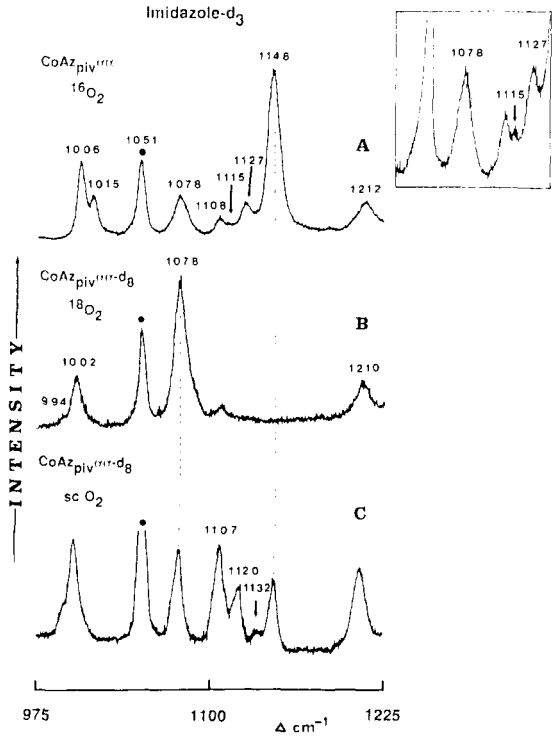

Figure 5. Resonance Raman spectra of O_2 adducts of $CoAz_{piv}\alpha\alpha$ complex with imidazole-d_3. See Figure 2 caption.

behavior observed in the RR spectra is thus the result of complicated vibrational mode coupling. Nevertheless, it is satisfying to point out that this complete set of complex data can be reasonably explained in an internally consistent manner by invoking vibrational coupling interactions among the specific modes of the various imidazole and O_2 isotopomer pairs.

Approximation of the bound dioxygen as a harmonic oscillator leads to an expected (oxygen) isotopic shift of 33 cm^{-1}. That is, given a $\nu(^{16}O-^{18}O)$ inherent frequency of 1111 cm^{-1}, the $\nu(^{16}O-^{16}O)$ and $\nu(^{18}O-^{18}O)$ are expected to occur at 1144 and 1078 cm^{-1}, respectively. The spectra of free imidazole and Im-d_1 (Figure 1) exhibit a band in the $\nu(^{16}O-^{16}O)$ region that is expected to shift up to $\approx$1150 cm^{-1} upon coordination.[19-21] Interaction of the $\nu(^{16}O-^{16}O)$ (inherent frequency = 1144 cm^{-1}) with this mode results in the appearance of two bands shifted by $\sim$6 cm^{-1} from their inherent frequencies; i.e., the 1144- and 1152-cm^{-1} modes shift to 1138 and 1158 cm^{-1} (Figures 2A and 3A). In both cases, the lower frequency component contains the major contribution of ν(O–O) and exhibits greater intensity. It is interesting to point out that even very subtle differences in these two spectra (Figures 2A and 3A) are consistent with this interpretation. Thus, in the case of Im-d_1 (Figure 3A), the $\nu(^{16}O-^{16}O)$ is 1 cm^{-1} lower than in Figure 2A and the 1156/1137 cm^{-1} intensity ratio in Figure 3A is greater than the 1158/1138 cm^{-1} ratio in Figure 2A. As was pointed out in our previous works,[10,13] the strength of the coupling is sensitive to energy matching of the coupled modes. On the basis of the spectra of Im and Im-d_1 shown in Figure 1, the Im-d_1 interacting mode is expected to be $\sim$2 cm^{-1} closer to $\nu(^{16}O-^{16}O)$ and should exhibit a slightly stronger interaction. This expectation is confirmed by the slightly greater shift of $\nu(^{16}O-^{16}O)$ of $\sim$7 cm^{-1} to 1137 cm^{-1} and slightly greater intensity of the internal ligand mode. Thus, the greater 1156/1137 cm^{-1} intensity ratio is predicted.

In the cases of free Im-d_2 and free Im-d_3, the strongest ligand modes occur at 1118 cm^{-1} (Figure 1C) and 1108/1119 cm^{-1} (Figure 1D). While these may shift slightly upon coordination, they are clearly in closer proximity to $\nu(^{16}O-^{18}O)$ than to $\nu(^{16}O-^{16}O)$ or $\nu(^{18}O-^{18}O)$. In both these cases then, strong coupling with $\nu(^{16}O-^{18}O)$ is expected. From inspection of Figures 2C and 3C, the inherent $\nu(^{16}O-^{18}O)$ is observed to occur at 1111 cm^{-1}. Coupling of $\nu(^{16}O-^{18}O)$ with the internal ligand mode of Im-d_2 gives rise to two bands located at 1106 and 1119 cm^{-1} (Figure 4C), implying an inherent frequency of 1114 cm^{-1} for coordinated Im-d_2 (i.e., a 5-cm^{-1} shift to higher frequency is expected on the basis of the 5-cm^{-1} shift to lower frequency observed for $\nu(^{16}O-^{18}O)$).

The situation for Im-d_3 is only slightly more complicated. The free-ligand spectrum (Figure 1D) exhibits two bands at 1108 and 1119 cm^{-1}. The presence of these two modes readily explains the complex spectroscopic behavior observed in Figure 5A,C. The strong $\nu(^{16}O-^{16}O)$ is shifted by only 3 or 4 cm^{-1} from its inherent frequency (1144 cm^{-1}) to 1148 cm^{-1} via interaction with the (coordinated) two ligand modes which show up as weak features at 1127 and 1115 cm^{-1}. Thus, the inherent frequencies of the coordinated Im-d_3 are probably 1130 and 1116 cm^{-1}.[10-13] These inherent frequencies also explain the behavior of the complex with scrambled O_2 isotopomers (Figure 5C). Thus, the $\nu(^{16}O-^{18}O)$, having an inherent frequency of 1111 cm^{-1}, is shifted down by 4 cm^{-1} to 1107 cm^{-1}, and both internal ligand modes are shifted up by 4 and 2 cm^{-1}, respectively, to 1120 and 1132 cm^{-1}; the one closer to $\nu(^{16}O-^{18}O)$ exhibiting the larger shift and stronger intensity. Note that the weak feature that appears near 1130 cm^{-1} in the traces 5A and 5C exhibits an apparent shift of 5 cm^{-1} (1127 to 1132 cm^{-1}). Such minor differences often are overlooked or cause confusion. It is thus especially satisfying to point out that systematic application of the vibrational coupling argument actually predicts this observed shift.

Finally, the behavior of $\nu(^{18}O-^{18}O)$ for the $^{18}O_2$ adducts is also readily explained by this interpretation. Thus, in the cases of Im-d_2 and Im-d_3 (Figures 4B and 5B), isolated symmetric bands are observed at 1078 cm^{-1}; i.e., at the predicted inherent frequency (based on the 1111-cm^{-1} bands in Figures 2C and 3C). As is seen in Figures 1C and 1D, Im-d_2 and Im-d_3 do not possess internal modes in this region; i.e., no vibrational coupling is expected in these cases. In the case of natural abundance imidazole, a mode is predicted to occur near 1060–1070 cm^{-1} (i.e., a slight shift upon coordination may occur). The spectrum shown in Figure 2A exhibits two bands at 1068 and 1082 cm^{-1}. These result from interaction of $\nu(^{18}O-^{18}O)$ (inherent frequency at 1078 cm^{-1}) with the imidazole mode whose apparent inherent frequency is 1072 cm^{-1} (i.e., induced shifts of $\pm$4 cm^{-1}). The Im-d_1 internal mode is expected near 1085 cm^{-1} (Figure 1B). Interaction of this with $\nu(^{18}O-^{18}O)$ gives rise to two bands at 1076 and 1089 cm^{-1}, implying an inherent frequency of the (coordinated) Im-d_1 mode at 1087 cm^{-1} (i.e., induced shifts of $\pm$2 cm^{-1}).

The preceding discussion employs a single concept (vibrationally coupled dioxygen) to provide a unified treatment that clarifies a large body of apparently complex spectral data. In fact, as we had pointed out in our previous work,[13] the spectroscopic patterns observed in the RR spectra of these O_2 adducts approximate that expected for coupled oscillators as discussed in standard references.[25] A quantitative treatment of the frequency perturbations and relative intensities of coupled modes for all of the O_2 adducts thus far studied,[10-13] as well as a discussion of the structural and electronic factors that dictate coupling strength in these systems, will be presented in a forthcoming article.[26] At this time it is only necessary to point out that, in the cases studied here, all of the observed frequency perturbations and approximate relative intensities of the various coupled partners are in good agreement with those calculated by using the equations given in ref 25.

In summary of this section, the ν(O–O) of the three dioxygen isotopomers vibrationally couple with internal modes of the trans-coordinated imidazole, giving rise to shifts of ν(O–O) from its inherent frequency and the appearance of weak secondary features associated with the imidazole internal modes. These latter features gain intensity as a consequence of the vibrational coupling with ν(O–O). When the inherent frequencies of the imidazole internal modes are altered by selective deuteriation, different vibrational patterns are observed. However, all of the observed

(25) Herzberg, G. *Molecular Spectra and Structure*; Van Nostrand Co.: New York, 1945; Vol. 2, p 215.
(26) Proniewicz, L. M.; Kincaid, J. R., submitted for publication.

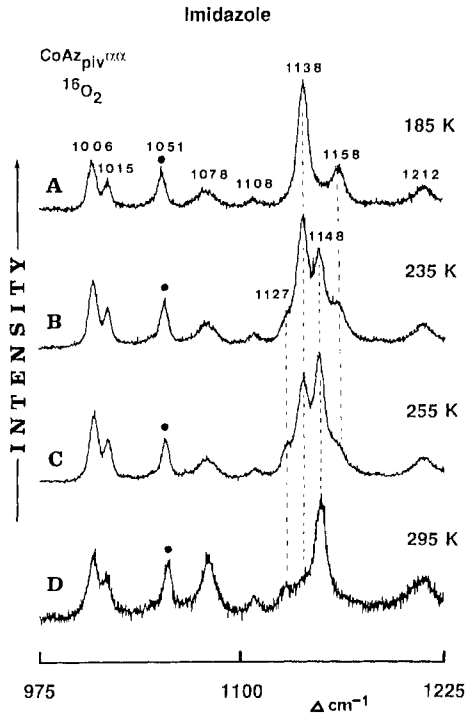

Figure 6. Resonance Raman spectra of the $^{16}O_2$ adduct of $CoAz_{piv}\alpha\alpha$ complex with imidazole. Imidazole concentration between 1×10^{-3} and 1×10^{-2} M. Temperatures measured as described in text.

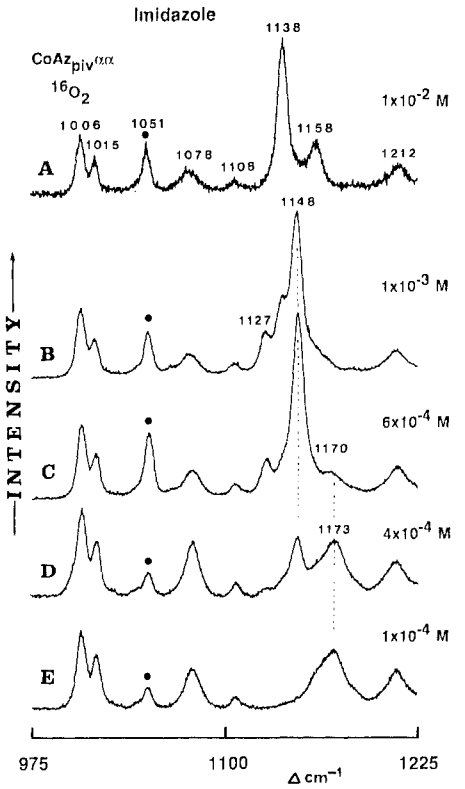

Figure 7. Resonance Raman spectra of the $^{16}O_2$ adduct of $CoAz_{piv}\alpha\alpha$ complex with imidazole. Temperature ~185 K; imidazole concentrations estimated as described in text.

frequency shifts in ν(O–O), as well as the exact positions and approximate intensities of the weak secondary features, are readily explained in terms of a vibrationally coupled dioxygen, the strength of the coupling depending on energy matching of the ν(O–O) with the interacting imidazole modes.[13,25,26]

2. Effect of Hydrogen Bonding of Coordinated Imidazole on the Vibrational Patterns of the Dioxygen Adducts. The highly protected cobalt porphyrin used in this study shields the bound dioxygen from interaction with solution components. This statement is supported by the fact that in the present study the $\nu(^{16}O–^{16}O)$ is not perturbed by the CH_2Cl_2 mode at 1156 cm^{-1}, whereas for corresponding complexes of unprotected porphyrins (such as CoTPP) the $\nu(^{16}O–^{16}O)$ is known to vibrationally couple with the internal mode of an associated CH_2Cl_2 molecule.[10–13] The elimination of direct interaction between bound O_2 and other solution components facilitates selective modulation of the properties of the bound imidazole by variation of solution conditions.

All of the studies described in the previous section were conducted in the presence of large excesses of imidazole, i.e., ligand concentrations of $\sim 10^{-2}$ M and cobalt porphyrin concentration of $\sim 5 \times 10^{-4}$ M. At this high concentration in nonprotic solvents imidazole is known to self-associate.[22–24] Thus, it is likely that the spectra shown in Figures 2–5 correspond to O_2 adducts in which the trans-coordinated imidazole is hydrogen bonded to excess imidazole present in the solution. Such interactions may be decreased or eliminated by increasing the temperature or decreasing the concentration of imidazole. The interesting spectral patterns shown in Figures 6 and 7 support this expectation.

In Figure 6 are shown the spectra obtained for the $^{16}O_2$ adduct of the natural-abundance imidazole complex, as a function of temperature. At 185 K the spectral pattern previously shown in Figure 2A is observed, i.e., two bands are observed at 1138 and 1158 cm^{-1} (Figure 6A). However, at room temperature (Figure 6D) these two bands have nearly disappeared, and new bands are seen at 1127 cm^{-1} (weak) and 1148 cm^{-1} (strong). At the two intermediate temperatures (traces B and C), both sets of bands are observed.

Essentially similar behavior is observed as the concentration of imidazole is varied (Figure 7). Thus, at an imidazole concentration of 1×10^{-2} M, the 1138/1158 cm^{-1} pair is dominant (trace A) while at 6×10^{-4} M imidazole, the 1127/1148 cm^{-1} pair dominates (trace C). It is interesting to note that at very low imidazole concentrations (traces D and E) a base-free dioxygen adduct is apparently formed as is evidenced by the appearance of an 1173-cm^{-1} feature that shifts to 1107 cm^{-1} in the case of $^{18}O_2$ [$\Delta\nu(^{16}O/^{18}O) = 66$ cm^{-1}]. The nature of this adduct, which also forms in the total absence of base, will be dealt with in a future paper. However, its appearance is peripheral to the present issue and will not be discussed further here.

The results presented in Figures 6 and 7 indicate that the O_2 adduct that has a hydrogen-bonded imidazole axial ligand gives rise to the 1138/1158 cm^{-1} pair while the non-hydrogen-bonded analogue is characterized by the 1127/1148 cm^{-1} pair of bands. To provide further support for this interpretation, we have included a study wherein a third solution component, which is known to hydrogen bond with imidazole,[24] is added. The spectra shown in Figure 8 demonstrate the effect of adding tri-*n*-octylphosphine oxide (TNOP) to a solution containing the $^{16}O_2$ adduct at low imidazole concentration. As is evident in the figure, the 1127/1148 cm^{-1} pair, characteristic of non-hydrogen-bound axial imidazole, is converted to the 1138/1158 cm^{-1} pattern upon the addition of TNOP. Obviously, this behavior is consistent with the contention that the 1138/1158 cm^{-1} pattern is characteristic of the hydrogen-bonded imidazole dioxygen adduct.

It is especially important to note that similar studies of *noncoupled* ν(O–O) do not show these effects. Thus, the $\nu(^{16}O–^{16}O)$ of the corresponding Im-d_2 complex (Figure 4A) is only weakly coupled, if at all. Variations of temperature or imidazole concentration, as well as addition of TNOP, all failed to alter the position of $\nu(^{16}O–^{16}O)$ (spectra not shown). Furthermore, similar variations of conditions failed to affect the behavior of $\nu(^{18}O–^{18}O)$ of the Im-d_3 analogue. We also wish to point out that both forms (i.e., the 1138/1158 and the 1148/1127 cm^{-1} species) exhibited identical frequencies for ν(Co–O), i.e., 520 cm^{-1}.

The most reasonable interpretation of the two distinctly different spectral patterns resulting from these controlled variations (temperature, imidazole concentration, and addition of TNOP) is that the inherent frequencies of the interacting imidazole internal modes are different for the two types of ligated imidazole. Thus, the

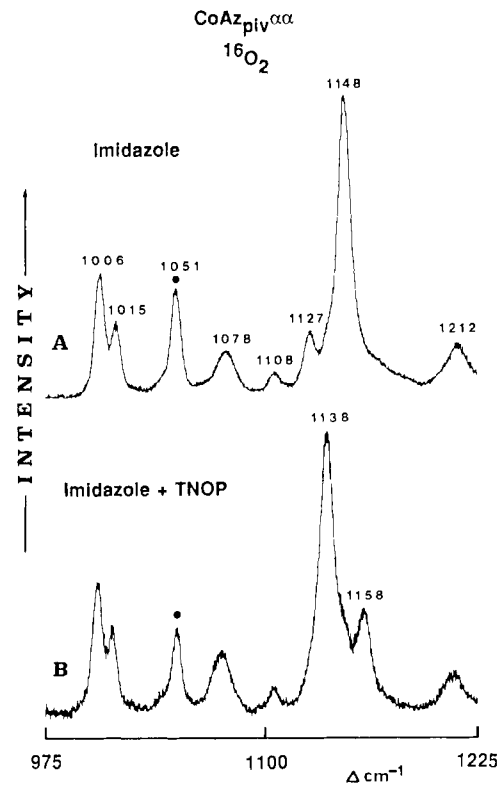

Figure 8. Resonance Raman spectra of the $^{16}O_2$ adduct of CoAz$_{piv}$αα complex with imidazole. The effect of tri-*n*-octylphosphine oxide (TNOP); imidazole concentration ~1 × 10^{-3} M, TNOP concentration ~5 × 10^{-2} M; temperature in both experiments ~185 K.

hydrogen-bonded form possesses an internal mode whose inherent frequency is 1152 cm^{-1}. Interaction of this mode with $\nu(^{16}O-^{16}O)$ at 1144 cm^{-1} gives rise to two bands observed at 1138 and 1158 cm^{-1} (i.e., +6 and −6 cm^{-1} shifts). The observation of a strong 1148-cm^{-1} feature, along with a weak secondary band at 1127 cm^{-1}, indicates that the non-hydrogen-bonded axial imidazole possesses an internal mode having an inherent frequency of 1131 cm^{-1}. Interaction of this mode with the $\nu(^{16}O-^{16}O)$ at 1144 cm^{-1} gives rise to two bands at 1127 and 1148 cm^{-1} (i.e., shifted by −4 and +4 cm^{-1} from their inherent frequencies). It is also satisfying to note that the strength of the interaction is greater for the former case where the inherent frequency difference is 8 cm^{-1} (1152 − 1144 cm^{-1}) than for the latter (inherent frequency difference is 13 cm^{-1} (1144 − 1131 cm^{-1})). That is, the observed frequency perturbations are 6 and 4 cm^{-1} respectively, and the 1158/1138 cm^{-1} ratio is larger than the 1127/1148 cm^{-1} ratio.

Finally, to conclude this section, it is important to emphasize that hydrogen-bond formation by the coordinated imidazole *does not* lead to changes in the inherent frequency of the ν(O–O) (or ν(Co–O)). The only consequence of such hydrogen bonding is the change in the observed spectral pattern that results from alteration of vibrational coupling of ν(O–O) with internal modes of the trans-coordinated imidazole. Such complicating interactions and the resulting complex spectral patterns underscore the need for a complete set of spectral data for isotopomeric species, as well as a range of solution conditions, to avoid incorrect inferences regarding structure and bonding changes. The implications of the present studies for interpretation of corresponding spectral data for cobalt-substituted hemeproteins are discussed below.

C. Implications for the Study of O_2 Adducts of Cobalt-Substituted Hemeproteins. In our earlier study of the O_2 adducts of cobalt-substituted hemeproteins we suggested that the complicated observed spectral patterns result from vibrational coupling of ν(O–O) with internal modes of the proximal (and possibly the distal) histidylimidazole.[10] We further pointed out that subtle changes in active-site structure and bonding may significantly affect the coupling parameters and lead to complex changes in the observed spectral patterns, emphasizing such issues as proximal imidazole hydrogen bonding, orientation of the proximal histidylimidazole plane with respect to the plane passing through the Co–N porphyrin axis, and hydrogen bonding of bound O_2 to the distal histidylimidazole fragment.

The present study is focused on the first of these issues and clearly demonstrates dramatic alterations in observed spectral patterns upon formation of a hydrogen bond between axially coordinated imidazole and other solution components. In fact, the present results confirm our previous suggestion[10] that even a chemically insignificant alteration can lead to a remarkably complex spectral perturbation. Thus, in the present work, hydrogen-bond formation at the imidazole NH does not lead to a change in the *inherent* frequency of ν(O–O) but does dramatically alter spectral patterns as a result of imidazole internal-mode changes.

The potential utility of such spectroscopic consequences in probing hemeprotein active-site structure depends ultimately on a better understanding of imidazole internal-mode structure and how it is affected by peripheral substituent (i.e., $-CH_2-$) disposition, hydrogen bonding, and coordinate-bond strength. While we and others are continuing efforts to identify conditions that lead to direct resonance enhancement of imidazole modes in the RR spectra of native hemeproteins, none have yet been identified and prospects are not hopeful (e.g., see ref 20). Thus, as was pointed out in our earlier report,[10] systematic analysis of the vibrational spectra of isotopically labeled histidylimidazole models and corresponding metal complexes will be required to provide the framework for a structural interpretation of the spectral patterns observed for O_2 adducts of the cobalt-substituted proteins.

The present studies do directly address the interesting proposal that hydrogen bonding at the proximal histidylimidazole can affect the strength of the metal–oxygen linkage in hemeprotein–O_2 adducts (ref 5 and references therein). Our results indicate that such interactions have no measurable effect on the *inherent* frequency of ν(O–O), i.e., in the uncoupled systems variation of imidazole concentration and temperature had not effect on $\nu(^{16}O-^{16}O)$, $\nu(^{18}O-^{18}O)$, or ν(Co–O). While the senstivity of the ν(O–O) response to such changes may be low and the strength of hydrogen bonding in our systems (i.e., self-association or association with TNOP) may be weaker than that present in the proteins, our results are in agreement with conclusions reached in a recent report by Traylor and Popovitz-Biro.[6] These workers showed that the O_2 affinity of a heme complex that possessed an internally hydrogen-bonded imidazole axial ligand was not significantly different from a non-hydrogen-bonded analogue.

D. Conclusions. The present study supports our earlier proposal[10] that internal modes of the proximal histidylimidazole are observed in the RR spectra of O_2 adducts of cobalt-substituted hemeproteins. The present results also confirm the suggestion made in the earlier work that subtle changes in structure and bonding in the heme pocket, such as variations in proximal imidazole hydrogen bonding, can lead to dramatic alterations in the observed spectral patterns. However, to the extent that ν(O–O) and ν(Co–O) are effective probes of metal–oxygen bond strength, the present results indicate that hydrogen bonding of the proximal imidazole has little effect on the metal–oxygen linkage, a conclusion that agrees with that made recently by Traylor and Popovitz-Biro.[6]

Acknowledgment. This work was supported by grants from the National Institute of Health (DK35153 to J.R.K.) and the National Science Foundation (DMB-8613741 to K.N. and CHE-8413956 to Marquette University). L.M.P. expresses his gratitude for Grant No. RP-II-13 provided by the Polish Ministry of Education.